that the stimulated small scale (SSS) model provided a better agreement with the experiment data than the Smagorinsky model.

The SSS model was utilized to describe the energy dissipation and the backscatter in the round jet was captured. The convective boundary condition at the outflow boundary ensured the less reflect on the upstream.

ACKNOWLEDGEMENTS

This project is supported by National Climbing Plan, National Foundation of Science , Doctoral Foundation of the National Education Committee and Hydrodynamic opening laboratory in Wuxi in P.R.China.

REFERENCES

1 Shah K.B. and Ferziger J.H. A new non-eddy viscosity subgrid-scale model and its application to channel flow. 1995, Center for Turbulence Research Annual Research Briefs.

2 Reynolds A.J. Observation of a liquid-into-liquid jet. J. Fluid Mech. 1962,14:552

3 Batchelor G.K and Gill A.E. Analysis of the stability of axisymmetric jets. J. Fluid Mech. 1962,14:529

4 Martin J.E. and Meiburg E. Numerical investigation of the three dimensionally evolving jets subjet to axisymmetric and azimuthal perturbations. J. Fluid Mech. 1991,230:271

5 Grinstein F.F and DeVore C.R. Dynamics of coherent structures and transition to turbulence in free square jets. Phys. Fluids 1997,8(5):1237

6 Akselvoll K. and Moin P. Large eddy simulation of turbulent confined coannular jets. J. Fluid Mech. 1996,315:387

7 Stanley S. and Sarkar S. Simulations of spatially developing two-dimensional shear layers and jets. Theoretical and computational fluid dynamics. 1997,9:121

8 Boersma B.J Brethouwer G. And Nieuwstadt F.T.M. A numerical investigate on the effect of the inflow conditions on the self-similar region of a round jet. Phy. Fluid 1998 10(4):899

9 Lowery P.S, Reynolds W.C. and Mansour N.N. Passive scalar entrainment and mixing in a forced, spatially developing mixing layer. 1987,AIAA-87-0132

10 Sami S., Carmody T. and Rouse H. Jet diffusion in the region of flow establishment. J.Fluid Mech. 1967,27:231

DIRECT NUMERICAL SIMULATION OF GÖRTLER INSTABILITY IN HYPERSONIC BOUNDARY LAYERS

C. W. WHANG AND X. ZHONG
Mechanical and Aerospace Engineering Department
University of California, Los Angeles, CA, 90095

1. Introduction

The transition of hypersonic boundary layer flow is one of the fundamental problems in fluid mechanics. In general, boundary layer flows become turbulent in three steps: 1) receptivity, 2) linear growth of disturbance, and 3) nonlinear effects in which the flow breaks down to turbulence. Görtler instability is one of many B-L instability mechnisms. Görtler vortices appear in boundary layer flow along concave surfaces due to the imbalance between pressure and centrifugal force. Many practical engineering designs involve concave surfaces such as engine inlet. Therefore, Görtler instability become an important subject in fluid mechanics.

For Görtler instability, it has been shown that the region of linear development of disturbances are relatively shorter than nonlinear developing region; therefore, nonlinear effects are mainly considered in Görtler instability. For nonlinear studies, Direct Numerical Simulation (DNS) which solve full Navier Stokes equations is an efficient method.

Previously there have been many DNS studies to solve nonlinear Görtler problems. Hall(1988) demonstrated that nonlinear evolution of streamwise Görtler vortices produces inflectional profiles which will presumably break down. Lee and Liu(1992) and Liu(1991) numerically showed mushroom like vortex due to nonlinear growth of Görtler vortices. Liu and Domaradzki(1993), Yu and Liu(1994), and Li and Malik(1995) studied secondary instability effects on Görtler vortices. Secondary instability is produced by interaction between TS waves and Görtler vortices.

Li and Domaradzki(1993) dealt with Görtler problem using Direct Numerical Simulation (DNS). Initial disturbances were obtained from Linear Stability Theory (LST) since initial stage of growing Görtler vortices is linear. They showed that Görtler vortices become turbulent due to the

spanwise velocity gradient as well as the normal velocity gradient. They mentioned that varicose mode of secondary instability is related to the normal velocity gradient and the sinuous mode is to the spanwise gradient and concluded that sinuous mode is dominant. Li and Malik(1995) used PSE (parabolic stability equation) method, and studied nonlinear effects of Grotler vortices. In their approach, they showed there are two kinds of secondary instability modes; even and odd. The even mode is related to the varicos mode, and the odd mode is to the sinous mode.

Most DNS works have considered simple geometry without shock and flat plate boundary layer mean flow. In this project, blunt body with bow shock which contains concave surface is considered, and 2-D mean flow is obtained from solving the full Navier Stokes equations. Görtler instability is investigated using two approaches: LST and DNS. Normal mode linear stability analysis is used for the initial disturbances for linear and nonlinear simulation and to verify the simulation code. DNS is used to simulate linear and nonlinear development of Görtler vortices in hypersonic boundary layers. Characteristics of nonlinear Görtler instability will be investigated.

2. Linear Stability Analysis

Although region for linear development of Görtler mode is much shorter than the nonlinear region, we can obtain lots of useful information from linear stability analysis. Along the concave surface, T-S wave (or shear mode) as well as Görtler mode exists. Parametric studies on the relative stability of Görtler and shear mode can be studied by LST. Linear stability analysis also help us to verify the numerical simulation code.

In the derivation of disturbance equations, we closely followed Malik's(Malik, 1990) formulation for cartesian coordinates. Coordinate transformation is applied to transform cartesian coordinates into curve linear system in order to include curvature effects.

The linear stability code for Görtler instability has been verified by comparing with available published papers(Whang *et al.*, 1999). Both shear and Görtler modes have been considered in the analysis. Unstable shear mode as well as Görtler mode exist along the concave surface; therefore, it is important to invetigate which mode is dominant. At hypersonic speed limit, second shear mode dominates the first mode; therefore Görtler modes and second shear modes are compared in the analysis.

Figure 1 shows the maximum temporal growth rates of Görtler and shear modes at constant Reynold's number (Re_δ) which is $\frac{U^*_\infty \rho^*_\infty \delta^*}{\mu^*_\infty}$ where δ^* is boundary layer thinkness. Each lines of Görtler modes indicates constant Görtler number (G) defined as $Re_\delta \sqrt{\frac{\delta}{R}}$. Reynold's number ($Re_\delta$) is fixed as 1500, and radius of curvature changes in order to study Görtler

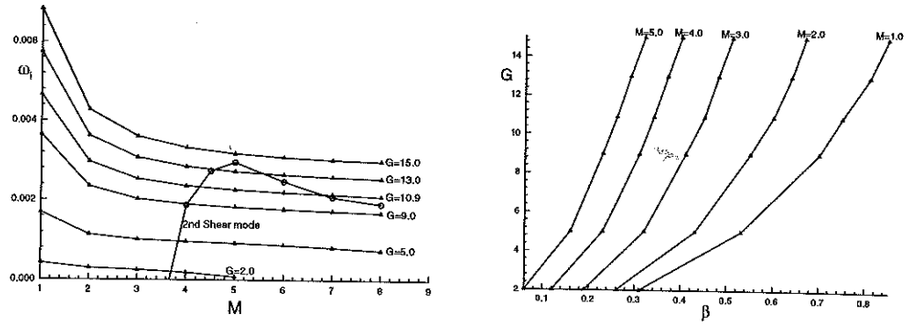

Figure 1. Comparison of the maximum growth rates of Görtler modes and second shear modes at $Re_\delta = 1500$. There is a critical Görtler number over which Görtler modes are dominant. Wavenumber, β, decreases as Mach number increases at fixed Görtler numbe.

number effects. As Görtler number increases, the maximum growth rates increase. Increasing Görtler number at fixed Reynolds number represents increase of curvature effects. As curvature increases, flow become more unstable(Whang *et al.*, 1999). It is also true for shear mode, but it does not affect the stability condition as much as for Görtler mode. Therefore in Fig. 1, second shear mode at $G = 15.0$ is only shown. The figure shows that there is a critical Görtler number over which Görtler mode dominates second shear mode at hypersonic speed limit.

At low mach number, Görtler modes dominate second shear mode. However, this is the region dominated by first shear modes which are not computed in this analysis. According to Mack's(Mack, 1984) results for flat plate at Re_δ=1500, we can roughly compare growth rates of Görtler modes and first shear modes. If Görtler number is greater than 15.0, Görtler modes dominate first shear modes.

Compressibility effects of Görtler modes are shown in Fig. 1. As Mach number increases, growth rate decreases. However, at hypersonic limit, stability effects of compressibility become less important. When Mach number is greater than 5, growth rates become constant. It is the same results as Spall and Malik(Spall *et al.*, 1983).

Figure 1 also shows relationship between spanwise wave number, β, which gives the maximum growth rates, and Mach number, M. As Mach number increases, the wave number decreases. El-Hady et al(El-Hady *et al.*, 1983) also mentioned this trend in their linear stability analysis.

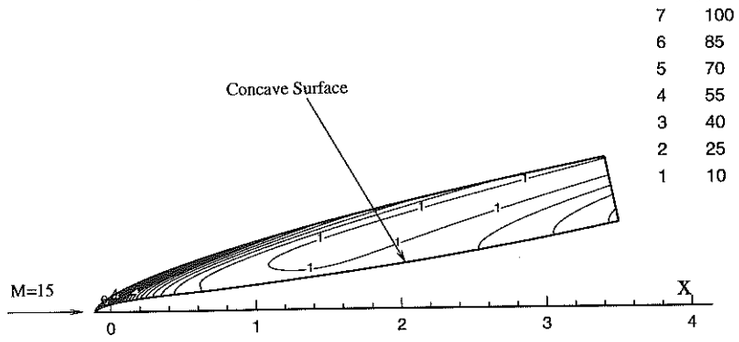

Figure 2. Pressure contours for the steady mean flow at $M_\infty = 15$, $T^*_\infty = 101.059$ K, $P^*_\infty = 10.3$ Pa, $T^*_w = 1000$ K, $Re_\infty = 150753.17$.

3. Görtler Vortices along Blunt Body with Concave Surface

3.1. 2-D MEAN FLOW

The steady flow solutions of the Navier-Stokes equations for the viscous hypersonic flow over blunt body is simulated using a fifth order explicit upwind scheme and shock fitting method(Zhong, 1997). Eight computational zones are used to carry out the simulation with a total of 1288 × 121 grids. Stretched grids are used in streamwise direction as well as in wall normal direction in order to resolve rapid changes of flow properties near the stagnation point in zone 1 and viscous layers. For other zones, streamwise stretching is not necessary; however, it is used in current analysis.

First three zones are parabolic blunt body, and concave surface is extended in the other zones. Using polynomial equations, we make continuous and smooth curves. At transition points between two polynomial equations, zeroth, first, and second order derivatives are matched; therefore, curves are continuous till second order derivatives. More smooth curves can be generated by matching the third order and more, but in our analysis, we matched till second order in order to get continuous radius curvature which is a function of first and second order derivatives. For the concave surface, we used large radius of curvature to avoid shock formation due to compressive waves inside the computational domains.

Freestream Mach number (M_∞) is 15. Temperature (T^*_∞) and pressure (P^*_∞) in freestream are 101.059 K and 10.3 Pa respectively. Unit Reynolds number, Re_∞, is 150753.175. The body surface is assumed to be a non-slip wall with an isothermal wall temperature $T^*_w = 1000K$.

Solutions of the steady mean pressure contours are shown in Fig. 2. Pressure is nondimensionalized by the flow variables in the freestream in

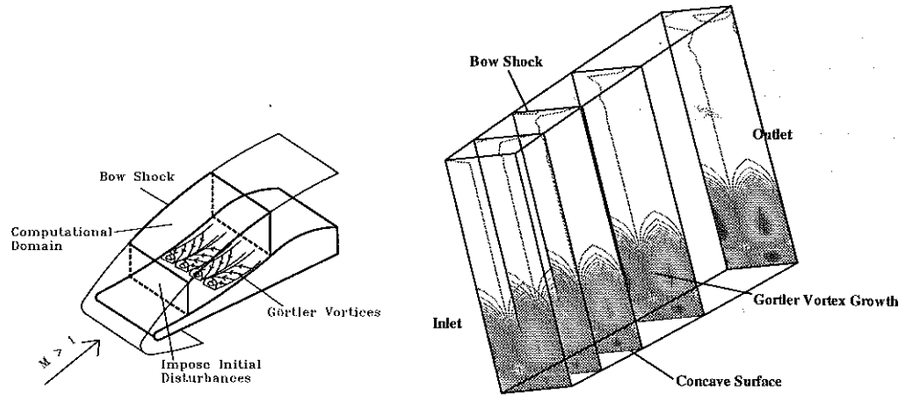

Figure 3. Temperature distribution of the primary Görtler modes along the streamwise direction at $G = 6.71$, $M = 7.89$, $Re = 4.23 \times 10^5$, and $\beta = 0.1$.

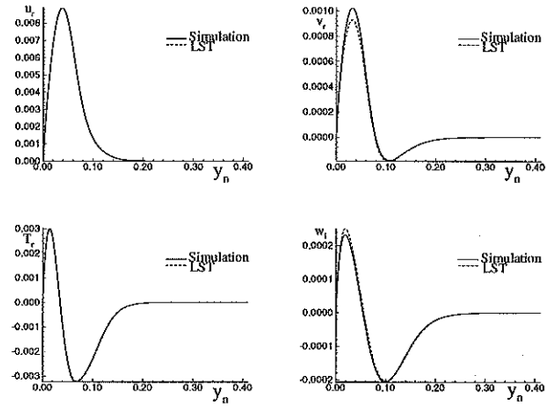

Figure 4. Distributions of imposed disturbances at I=100 of zone 7 at $G = 6.71$, $M = 7.89$, $Re = 4.23 \times 10^5$, and $\beta = 0.1$. Results are compared with LST results.

front of shock. The figure shows the effect of concavity on the pressure field. Concave wall starts when x is approximately 0.5m, and flow properties change after that point.

3.2. CASE I: LINEAR GROWTH OF GÖRTLER VORTICES

Simulation code can be verified by comparing simulated results with those obtained from linear stability analysis. 3-D disturbed flow is computed using 2-D mean flow. Concave surfaces are included in zone 4-8. Calculated

Görtler number is between 2.5 to 10.9, and Mach number behind shock is in the range of 6 to 8.9. Since Görtler number is relatively low at such high Mach number, zone 4 and 5 do not have unstable modes according to LST calculation. Görtler mode becomes unstable in zone 6. Disturbances are imposed in inlet of zone 7. Inlet Görtler number (G) and Reynolds number (Re_x) are 6.71 and 4.23×10^5. Inlet disturbances of the primary Görtler modes are obtained from linear stability analysis using the simulated mean flow.

Inlet boundary conditions are

$$\begin{aligned} u &= \overline{U}(x,y,z) + \epsilon\hat{u}_r(x,y,z,t)\cos(\beta z) \\ v &= \overline{V}(x,y,z) + \epsilon\hat{v}_r(x,y,z,t)\cos(\beta z) \\ w &= \overline{W}(x,y,z) - \epsilon\hat{w}_i(x,y,z,t)\sin(\beta z) \\ p &= \overline{P}(x,y,z) + \epsilon\hat{p}_r(x,y,z,t)\cos(\beta z) \\ T &= \overline{T}(x,y,z) + \epsilon\hat{T}_r(x,y,z,t)\cos(\beta z) \quad , \end{aligned} \tag{1}$$

where $\hat{u}_r$, $\hat{v}_r$, $\hat{w}_i$, $\hat{p}_r$, anf $\hat{T}_r$ are eigenfunctions obtained from LST. Other eigenfunctions ($\hat{u}_i$, $\hat{v}_i$, $\hat{w}_r$, $\hat{p}_i$, anf $\hat{T}_i$) are zero. Since steady Görtler vortices are observed in experiments, we study spatial Görtler instability. In spatial linear stability analysis, ω is zero; therefore, eigenfunctions do not depend on time, and initial disturbances at inlet of zone 7 are fixed as time changes. Inlet disturbances propagates spatially and converged to steady state condition.

We used four points in z-direction to cover one wavelength of spanwise disturbances. Spectral method is applied to spanwize direction to get accurate results. Wavelength is calculated from wavenumber β. In the current computation, β, which is nondimensionalized by boundary layer thickness, δ, is 0.1. It gives maximum growth rate of Görlter mode.

To verify Navier Stokes solver, simulated results are compared with those obtained from LST. We set ϵ is 0.001 which makes disturbances grow linearly. Figure 3 shows the temperature perturbation contours of primary Görtler modes along the streamwise direction. The perturbation contains two peaks along wall normal direction. The growth of the Görtler vortices in the streamwise direction is shown by the intensity of the disturbances. Figure 4 show distributions of simulated disturbances in normal direction at later station. y_n indicates the wall normal distance. LST results are also plotted in the same figures. The results show a good agreement between LST and Navier Stokes results.

3.3. CASE II : NON-LINEAR GROWTH OF GÖRTLER VORTICES

It is an important topic how Görtler vortrices break down to turbulence. Experiments showed that it is mainly due to the interaction of nonlinear

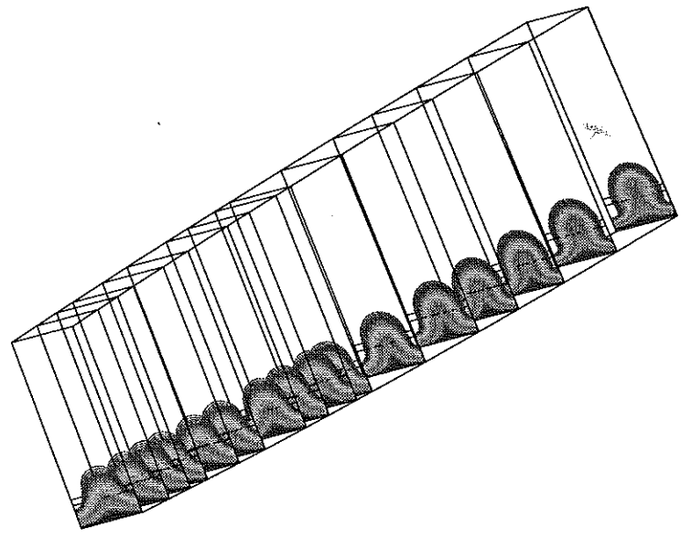

Figure 5. Distributions of iso-contours of streamwise mean velocity along the streamwise direction. The size of grids is $321 \times 121 \times 16$. Mushroom shaped vortices develop.

growth of Görtler vortices and other forms of disturbances. In nonlinear growing process, mushroom shaped vortices are produced since the counter-rotating vortices pump fluid with a low streamwise velocity away from the wall. There are two regions in Görtler vortices which are peak (low velocity region) and valley (high velocity region). These two regions produce the mushroom shaped vortices. Interaction between these vortices and traveling wave is the main factor of breking down to turbulencs.

To study nonlinear effects of Görtler instability, large amplitude disturbances are introduced at inlet of zone 7. The amplitude of the initial Görtler vortices is about $0.3U_\infty$. Two zones (zone 7 and zone 8) are used in nonlinear simulation. Mach number behind shock is between 7.89 to 8.92. Renold's number (Re_x) is in the range of 4.23×10^5 to 8.49×10^5. Each zones are resolved by $161 \times 121 \times 16$ grids. In the simulation, parallel computing is applied to reduce the computational time. Six nodes are applied to each zones.

Figure 5 shows distributions of streamwise velocities as flow moves downstream. The development of mushroom shaped vortices is well represented in the figure. Bow shock does not have much effects on flow field. The iso-contours of streamwise mean velocity at four different streamwise locations are shown in figure 6. Peak and valley regions are clearly shown. While the middle region (peak) tends to go up, others becomes narrower.

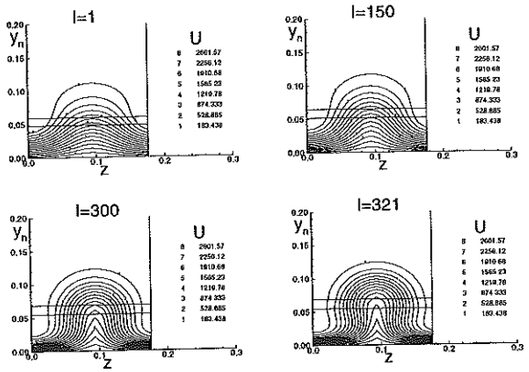

Figure 6. Iso-contours of the mean streamwise velocity in the cross-stream plane for several streamwise locations.

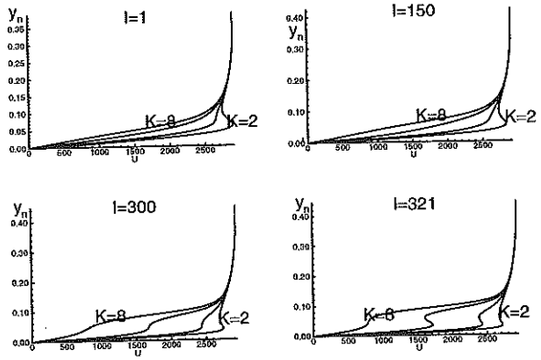

Figure 7. Profiles of the streamwise velocity in the vertical direction at four different streamwise locations. Velocity of the peak region (K=6) near the wall increases as flow moves downstream.

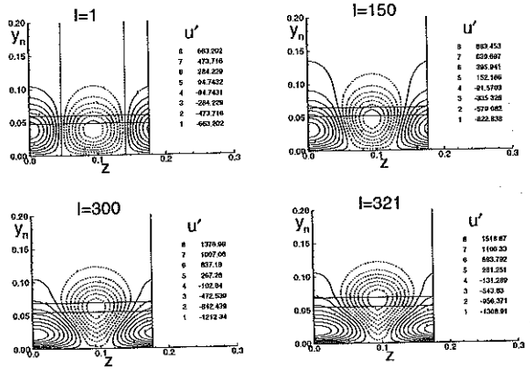

Figure 8. Streamwise velocity disturbance contours at four different streamwise locations. Disturbances in valley region moves to the peak region of Görtler vortices.

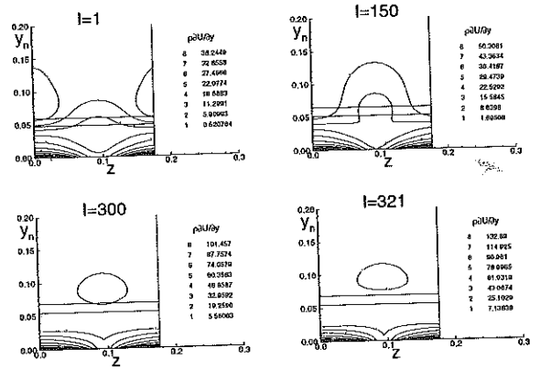

Figure 9. Iso-contours of normal gradient of the mean streamwise velocity in the cross-stream plane for several streamwise locations.

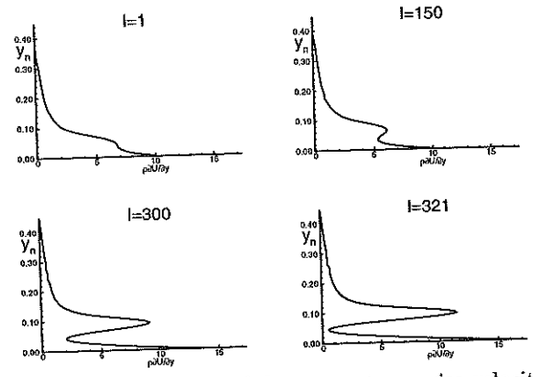

Figure 10. Profiles of normal gradient of the mean streamwise velocity in the vertical direction at peak region. Inflection points develop along the streamwise direction.

Profiles of the streamwise velocity in the vertical direction at four different spanwise locations are shown in Fig. 7. Velocity in peak region increases near the wall, and inflection points develop. Liu and Domaradzki(1993) mentioned that the Görtler vortices pump vertically the low-speed fluid away from the wall in the peak region and push the high speed fluid toward the wall in the valley region. However, there is the limitation of growing thinkness of the peak, and high speed fluid starts to tranfer to the peak region, and mushroom shaped vortices are produced. Streamwise velocity perturbation contours shown in Fig. 8 represent fluid near the wall in peak region is transfered to the valley.

In Görtler instability, inflection points develop in wall normal and spanwise directions, and inviscid instabililty problem become important. Derivatives of the streamwise velocity show cleart development of inflection points.

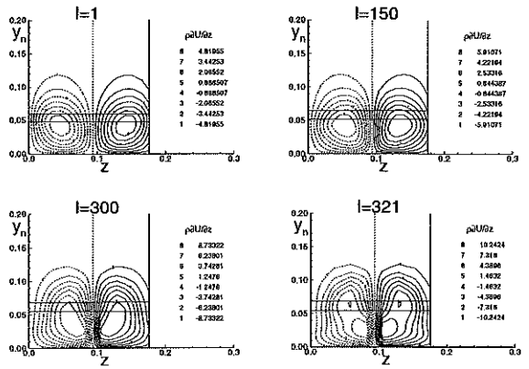

Figure 11. Iso-contours of spanwise gradient of the mean streamwise velocity in the cross-stream plane for several streamwise locations

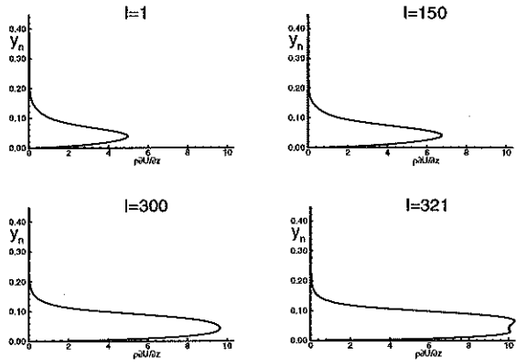

Figure 12. Profiles of spanwise gradient of the mean streamwise velocity in the vertical direction at peak region. Inflection points develop along the streamwise direction.

Figure 9 shows iso-contour of $\rho\frac{\partial U}{\partial y}$ in four different streamwise locations. Structure in peak region (low velocity region) changes as the flow moves. The vertical shear has its maximum in the low velocity region. Distributions of the normal streamwise velocity gradients at the spanwise location, in which the magnitude of $\rho\frac{\partial U}{\partial y}$ is the maximum, are shown in Fig. 10. Inflection points develop in the peak region. The magnitude increases as the flow moves which means that effects of inflection points increase.

Figure 11 and 12 show profiles of spanwise velocity gradients, $\rho\frac{\partial U}{\partial z}$, at four different streamwise locations. Both figures also represent the development of inflection points. Inflectional profiles appear in spanwise direction as well as normal direction, and they are related to secondary instability which is inviscid instability. Using energy conversion mechanism, Yu *et al.*(1994) showed that sinuous mode of secondary instability is related to normal velocity gradient, and various mode is related to the spanwise gradient.

4. Summary

In this paper, linear and nonlinear development of Görtler vortices were investigated. Parametric studies on relation between Görtler and shear modes were considered by linear stability analysis. At hypersonic speed limit, the maximum growth rates of Görtler and shear modes were computed. Mach number varied 1 to 8, and Re_δ is fixed as 1500. There is a critical Görtler number over which Görtler modes are dominant. Increase of Görtler number indicates increase of concave surface effects. Concavity destabilizes the flow, but it affects more Görtler modes than shear mode. Changing curvature causes dramatic changes in growth rate of Görtler mode but little changes for the second shear mode.

Mean flow along the blunt body which includes concave wall was simulated by a fifth-order explicit unsteady computer code. It showed the effect of concavity on the pressure field. Disturbances computed by the stability code were added in inlet of zone 7. Simulation results were compared with results predicted by LST. There were good agreements between two results.

Finally we studied nonlinear effects of Görtler vortices. Simulation showed the development of high and low velocity regions in Görtler vortices. The transfer of high speed fluid in valley region into the peak produced mushroom shaped vortices. Inflection points developed in nonlinear growth of Görtler vortices. The profiles of normal and spanwise velocity gradient showed the inflectional points which induce the inviscid instability problem.

5. Future Works

Work is in progress to include bow shock effects, nose bluntness and more detailed studies on nonlinear Görtler instability. To study bow shock effects on Görtler instability, boundary layer flow without shock will be investigated. Nonlinear study of Görtler instability includes interactions with other forms of disturbances(eg. TS waves, cross flow effects etc.) and mixing effects when fuel injection is applied in front of engine inlet.

6. Acknowledgments

This research was supported by the Air Force Office of Scientific Research under grant number F49620-97-1-0030 monitored by Dr. Len Sakell.

References

El-Hady, N.M. and Verma, A.K. (1983) Growth of Görtler Vortices in Compressible Boundary Layers along Curved Surfaces, *J. Engineering and Appl. Sciences* **Vol. 2**,pp. 213–238

Hall P.(1988) , The nonlinear development of Görtler vortices in growing boundary layers, *J. Fluid Mech.* **Vol. 193**,pp. 243–266

Lee K. and Liu J. T. C.(1992) , On the growth of mushroomlike structure in nonlinear spatially developing Görtler vortex flow, *Phys. Fluids* **Vol. 4(1)**,pp. 95–103

Li F. and Malik M. R.(1995) , Fundamental and subharmonic secondary instabilities of Görtler vortices, *J. Fluid Mech.* **Vol. 297**,pp. 77–100

Liu J. T. C.(1991) , On scalar transport in nonlinearly developing Görtler vortex flow *Geophys. Astrophys. Fluid Dynamics* **Vol. 58**,pp. 133–145

Liu W. and Domaradzki J. A.(1993) , Direct numerical simulation of transition to turbulence in Görtler flow, *J. Fluid Mech* **Vol. 246**,pp. 267–299

Mack, L.M. (1984) Boundary layer linear stability theory, *AGARD Rep. No. 709*

Malik, M.R. (1990) Numerical methods for hypersonic boundary layer stability, *J. Comput. Phys.* **Vol. 86**,pp. 376–413

Spall, R.E. and Malik, M.R. (1989) Görtler Vortices in Supersonic and Hypersonic Boundary Layers, *Phys. Fluids* **Vol. 1(11)**,pp. 1822–1835

Whang, C.W. and Zhong, X. (1999) Direct Numerical Simulation of Görtler Instability in Hypersonic Boundary Layers, *AIAA paper 99-0291*

Yu X. and Liu J. T. C.(1994) , On the mechanism of sinuous and varicose modes in three-dimensional viscous secondary instability of nonlinear Görtler rolls, *Phys. Fluids* **Vol. 6(2)**,pp. 736–750

Zhong, X.(1997) Direct numerical simulation of hypersonic boundary-layer transition over blunt leading edges, partI: a new numerical method and validation, *AIAA paper 97-0755.*

STUDY ON TRANSPORTATION OF PASSIVE SCALAR IN SHEARLESS MINGING LAYER BY LARGE EDDY SIMULATION*

ZHANG Zhaoshun and CHEN Yu Guang and CUI Guixiang and XU Chunxiao
Department of Engineering Mechanics, Tsinghua University, Beijing CHINA
L. SHAO and J.P. BERTOGLIO
Laboratory of Fluid Mechanics and Acoustics, Ecole Centrale de Lyon, FRANCE

1. INTRODUCTION

The turbulent transportation of mass and energy is of great importance in engineering and natural environment. Classic theories of turbulent transportation of passive scalar in isotropic turbulence have been proposed by Oboukhov[1] and Batchelor[2], etc. However, recent experimental and numerical studies show that intermittence appears in passive scalar fluctuations while the fluid turbulence is isotropic and its PDF is Gaussian[3], [4]. Therefore it is worth to have detailed study of the transportation of passive scalar in turbulence from either theoretical or practical view. In this paper we focus on the problem of transportation of passive scalar in the inhomogeneous turbulence and take the homogeneous turbulence case as an example for verification. The shearless mixing layer is an ideal case for studying the turbulent transportation process without the influence of the instability mechanism introduced by mean shear. Experimental results of transportation of passive scalar in shearless mixing layer have been provided by Veeravalli and Warhaft (1989)[5] and they are good resources for verification of numerical study. Both direct numerical simulation (DNS) and large eddy simulation (LES) are good choices for better understanding of the mechanism and prediction of quantitative properties in the turbulent transportation. For instance, the entrainment in a decaying shearless mixing layer was studied by Brigg et al.[6] at Reynolds number of 40 based on the Taylor microscale λ and $q=\sqrt{u_i u_i}$ by use of DNS. For the investigation of turbulent transportation of inhomogeneous passive scalar field, e.g. the concentration and temperature, a line source or sheet source of passive scalar is a good testing case in both homogeneous and inhomogeneous turbulence. Experimental results for the turbulent transportation of a line source in shearless turbulent mixing layer are also available (Veeravalli and Warhaft, 1990)[7]. We applied LES to the investigation of the turbulent transportation of passive scalar in the inhomogeneous turbulence. We found great intermittence of velocity fluctuation in the shearless mixing layer previously[8] and we will disclose that much greater intermittence of passive scalar fluctuations also occurs in the shearless mixing layer. The great intermittence of passive scalar results in the increment of the mean flux of passive scalar, which is important in prediction of the heat and mass transfer in engineering and environment.

2. PHYSICAL MODEL AND NUMERICAL METHOD

The shearless mixing layer is composed of two blocks of homogeneous turbulence with different length scales and kinetic energy, the initial velocity fluctuations in the two blocks, as shown in Figure 1, are homogeneous and nearly isotropic. The initial temperature distributions can be imposed in different profiles, such as pure random with zero mean, constant gradient with or without fluctuations and a plane source which is simulated by a Gaussian function with small variance. The mixing process takes place between two blocks of the shearless mixing layer while the mixing region is expanding. In this paper we put a plane sheet

* A project co-sponsored by CNNSF(19732005), Chinese Ministry of Science and Technology LIAMA and Dassault Aviation